Contribution from the Department of Chemistry,
The University of Chicago, Chicago, Illinois 60637

Electronic Control of the Geometry of Rutile and Related Structures

JEREMY K. BURDETT

Received October 26, 1984

The electronic structure of the rutile arrangement and those of some of its distorted variants are studied by using tight-binding calculations on the crystalline materials and molecular orbital computations on fragments torn from the crystal lattice. The essential difference between the oxides and the chalcogenides and heavier halogens lies in the efficient stabilization of the planar AM_3 unit for A = O but not for A = S, Cl, etc., by the metals acting as good π acceptors. Thus the rutile structure is found for oxides but the cadmium halide structure for heavier atoms A. The energetics of one structure relative to another at d^0 are readily understood in terms of the competing effects of the anionic lattice (a matrix effect) and the local angular geometric preferences of the anion and cation. The distorted rutile arrangements of the MoO_2 and β-ReO_2 types may be energetically discriminated by using a simple result from the method of moments.

Introduction

The two most common structural types for MX_2 systems containing six-coordinate metal and three-coordinate X atoms are the rutile and cadmium iodide types, usually described in terms of eutactic[1] arrangements of X atoms where half of the octahedral holes are occupied. The phrase "rutile type" is often used to describe structures where, although the atomic connectivity of the atoms is the same, local geometrical variations are significant. For example, pairing of the metal atoms, as in the MoO_2 variant, reduces the symmetry from tetragonal to monoclinic, and requiring the anions to be in hexagonal eutaxy gives the orthorhombic $CaCl_2$ type. In this paper we will investigate the electronic forces responsible for stabilizing one variant over another and also examine the more general question of the factors influencing the stability of the rutile over cadmium iodide arrangement for oxides and fluorides but the converse for chalcogenides and heavier halides. Although we will use the terms anion and cation to identify the more electropositive and electronegative atoms, respectively, we do not intend this usage to convey any commitment to an ionic model. In fact, the ideas we will present will be supported by tight-binding calculations for the crystalline solids and molecular orbital computations for small fragments. In both we will use the extended Hückel ansatz where such Coulombic forces are not explicitly included. One of our aims, both here and elsewhere,[2] will be to see how the actual geometry of these solids is set by the interplay of local geometric effects and the energetics of the anionic lattice. The idea of such a "matrix effect" in determining the details of structures has been examined in qualitative terms by Corbett[3] with reference to several metal–metal-bonded species. A systematic picture emerges concerning the geometrical features of early-transition-metal systems once it is included. The distortion of the Chevrel phases from the idealized to the observed structure contains a strong matrix component, which we have been able to assess numerically.[4] O'Keeffe has suggested[1b,5] that the structure of many "ionic" materials (rutile included) is the one of maximum volume subject to the constraint of a fixed anion–cation distance. Here the anion–anion repulsions (implicitly assumed to be Coulombic in nature) are minimized.

The Undistorted Rutile Structure

The rutile (TiO_2) structure is shown in Figure 1. It is a tetragonal variant of the orthorhombic $CaCl_2$ type, which belongs to the space group *Pnnm* with the Ca atoms in 2(a) (0, 0, 0; $^1/_2$, $^1/_2$, $^1/_2$) and the Cl atoms in 4(g) ($\pm(u, v, 0; u + ^1/_2, ^1/_2 - v, ^1/_2)$). Table I shows how variation of these parameters gives rise to some closely related structures. If $u = v$, then the rutile structure results. The cations are in octahedral coordination (although not necessarily regular). Geometrically the structure may be described (**1**)

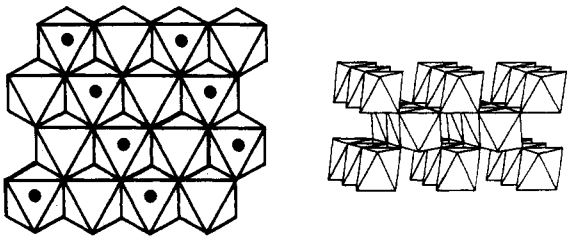

1

as a distorted hexagonal eutactic array of oxide ions in which half of the octahedral voids in each layer are occupied by metal atoms such that straight chains of edge-sharing octahedra (two edges shared per octahedron) lie parallel to the z axis of the tetragonal cell. For an ideal hexagonal eutaxy of anions, the anion coordination environment is simply derived from that of the trigonal prism (**2**) with three vacancies as shown in **3**. The resulting

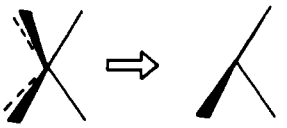

2 **3**

geometry is nonplanar with angles shown in **4**. If $u = v$ (rutile

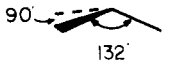

4

structure), then this unit is planar. The volume of the orthorhombic arrangement[1b] is given by

$$V^2 = l^6\beta^2(4u + 4\beta^2 v - 1 - \beta^2)/(u^2 + \beta^2 v^2)^3 \qquad (1)$$

if all A–X bonds are fixed equal to l. In this case

$$\gamma^2 = 4u + 4v\beta^2 - 1 - \beta^2 \qquad (2)$$

The rutile structure with this restriction (and with $u = v$, $\gamma = 1$) thus has one degree of freedom, which we will define by variation of u. The maximum volume structure from eq 1 occurs for the tetragonal rutile geometry with $u = 0.300$ and $\gamma = 0.632$. Figure 2 shows how the calculated energy for TiO_2 has a minimum close to the geometry with maximum volume and close to the observed arrangement. (The geometrical and orbital parameters used in our calculations are given in the Appendix.) The latter has Ti–O distances that are not all equal (there are four short and two long linkages), but a calculation on the observed geometry with an average bond length the same as that used in Figure 2 gives an energy close to that of the energy minimum in this figure. We have also calculated the energetics of the oxide lattice alone (assuming a charge of 2– on each oxygen atom) and that associated with TiO_6^{8-} and OTi_3^{10+} "molecules" during these geometrical changes. In such units interactions between the ligands were switched off so that the effects we measure represent the

(1) (a) We use this expression to define a packing of atoms whose centers are arranged as the centers of hard spheres in closest packing.[1b] In this way we avoid that nebulous concept of "ionic size". (b) O'Keeffe, M. *Acta Crystallogr., Sect. A: Cryst. Phys., Diffr., Theor. Gen. Crystallogr.* **1977**, *A33*, 924.
(2) Burdett, J. K.; Caneva, D. *Inorg. Chem.*, in press.
(3) Corbett, J. D. *J. Solid State Chem.* **1981**, *39*, 56; **1981**, *37*, 335.
(4) Burdett, J. K.; Lin, J.-H. *Inorg. Chem.* **1982**, *21*, 5.
(5) O'Keeffe, M. In "Structure and Bonding in Complex Solids", O'Keeffe, M., Navrotsky, A., Eds.; Academic Press: New York, 1981.

0020-1669/85/1324-2244$01.50/0

Table I. Geometrical Data for Rutile-like Structures

name	u	v	b/a (=β)	c/a (=γ)	M–M dist,[a,e] Å	M–O–M,[b,f] deg
$CaCl_2$ (obsd)	0.275	0.325	1.030	0.673		
PtO_2 (obsd)[c]	0.281	0.348	1.010	0.699		
hexagonal eutaxy	1/3	1/4	8/3 (0.943)	$1/3^{1/2}$ (0.577)	2.76	
rutile (max vol)	0.30	0.30	1.0	$(2/5)^{1/2}$	2.91	96
rutile (elec min)	0.315	0.315	1.0	0.721	3.16	108
rutile (reg oct)	0.293	0.293	1.0	0.66	2.76	90
rutile (obsd)[c]	0.305	0.305	1.0	0.634	2.8[d]	95

[a] Ti–O distance = 1.95 Å. [b] For the planar OTi_3 unit in a tetragonal space group. [c] Inequivalent M–O distances. [d] Assuming an average Ti–O distance of 1.95 Å. [e] For comparison with other structures discussed later: cadmium iodide 2.76 (regular), 2.82 (flattened), 2.70 Å (elongated); MoO_2 (average Ti–O distance of 1.95 Å) 2.47, 3.03 Å. [f] The angles in an idealized MoO_2 structure are 78 and 102°.

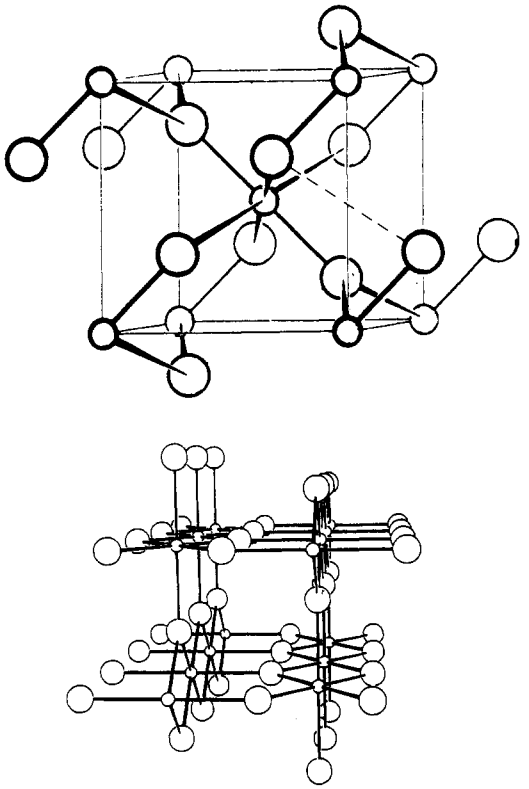

Figure 1. The rutile structure.

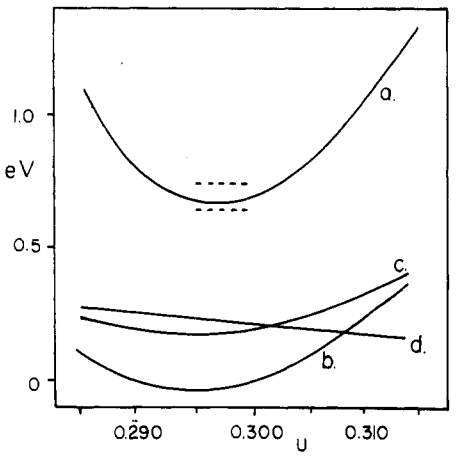

Figure 2. Energetics of distortion of TiO_2 in the rutile structure as a function of u, on a model where all Ti–O distances are fixed at 1.95 Å: (a) full tight-binding calculation on TiO_2 (energy per Ti_2O_4 unit); (b) tight-binding calculation for the oxide ions only of part a (energy per $\square_2O_4$ unit); (c) molecular orbital calculation on a TiO_6^{8-} unit; (d) molecular orbital calculation on an OTi_3^{10+} unit (energy per Ti_2O_4 unit). Only relative energy changes are shown in this picture. The two dashed lines represent the energy of structures where the Ti–O distances are not all equal. They have been scaled so that the average Ti–O distance is 1.95 Å. The dashed line that lies to higher energy represents the structure where the Ti–O distances are changed in the sense of the observed structure. The dashed line that lies to lower energy represents a distortion of the opposite sense.

result of geometry variations on local "anion–cation" interactions and the influence of the anion lattice is not double-counted when these local effects are added together as an estimate of the total energy variation. The local metal geometry is energetically best in a regular octahedral arrangement (u = 0.293) and the oxygen atom prefers a trigonal-planar geometry, but the energetic variation with u of these energetic contributors is relatively small and the location of the lowest energy structure seems to be dominated by the energetics of the ion array. The energetic details are given in Table II. Notice that the estimate of the energetic variation of the total energy with u is generally smaller than that calculated by using a full tight-binding calculation on the TiO_2 crystal. This is in spite of the fact that the energetics of the oxide ion matrix is probably overestimated since a full charge of 2– is assumed in the relevant tight-binding calculation. In using the energetics of the fragments, we obviously have not taken into account metal–metal interactions either. These may be of the direct type or occur by through-bond coupling via the oxide lattice. The structure we calculate to be of lowest energy is then the one that minimizes O–O repulsions within the constraint of a fixed metal–oxygen distance. Our anionic repulsions however are simply the overlap repulsions associated with the closed shells of electrons. (Figure 3 shows how the energy of a pair of O^{2-} ions varies with their internuclear separation. These are results from a molecular orbital calculation that used the same parameters as in all the other computations.) Notice that the minimum predicted by electrostatic reasoning[6] (u = 0.315) is energetically of high energy. From

Table II. Energetic Contributions (eV) to d^0 TiO_2 for Selected Structures[a]

structure	E(I)	E(II)	E(III)	E(IV)	E(V)
rutile (max vol)[b]	0.0	0.0	0.0	0.0	0.0
rutile (elec min)[c]	0.786	0.358	0.097	–0.012	0.504
rutile (u = 0.293)[d]	–0.005	–0.012	–0.002	0.018	0.056
rutile (obsd)	0.055	0.016	0.004	0.001	0.028
rutile (lowest energy)[e]	–0.047	–0.007	–0.005	–0.001	–0.021
rutile (hex eut)	0.146	0.017	0.002	0.038	0.177
anatase (obsd)	0.422	0.129	0.024	0.038	0.329
α-PbO_2 (obsd)	0.769	0.364	0.060	0.006	0.496
CdI_2 (regular)	1.492	0.019	0.002	0.359	1.459
CdI_2 (flattened)	1.379	0.044	0.005	0.329	1.370
CdI_2 (elongated)	1.646	0.027	0.001	0.386	1.573
MoS_2	2.429	0.553	0.053	0.391	2.223
SiO_2 (obsd)[f]	0.109	0.087	0.0	0.0	0.087
SiO_2 (opp obsd)[f]	0.048	0.092	0.0	0.0	0.092

[a] The energies are relative to that of the maximum-volume rutile structure with all Ti–O distances equal. The energetic contributors E(I)–E(V) are defined as follows: E(I), energy from TiO_2 tight-bonding calculation (per $(TiO_2)_2$); E(II), energy from tight-binding calculation on the oxide lattice (per $(\square O_2)_2$); E(III), energy from molecular orbital calculation on TiO_6^{8-}; E(IV), energy from molecular orbital calculation on OTi_3^{10+}; E(V), estimate of total energy variation from a summation of the energetics of the ion array and local geometry contributions. [b] u = 0.300. [c] u = 0.315. [d] u = 0.293 corresponds to exactly regular TiO_6 octahedra. [e] This is a distortion in exactly the opposite sense to the observed one. [f] These entries are for SiO_2 itself.

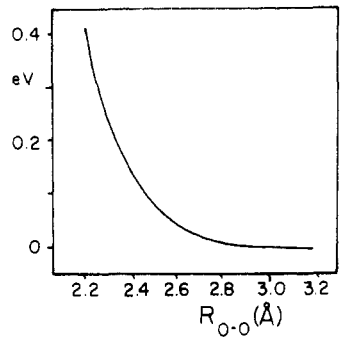

Figure 3. Repulsion curve between two O^{2-} ions as a function of internuclear distance computed by using a molecular orbital calculation (energies per four oxygen atoms).

Table II we can see that this is largely the result of unfavorable anion–anion interactions. This is due to the simple fact (shown in **5**) that the shared-edge O–O distance is short and (from Figure

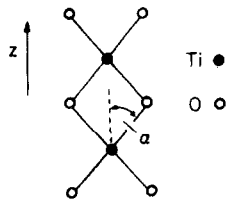

5

3) energetically unfavorable. (Pauling[7] also recognized that here lay the failure of the simple ionic model for rutile. By inclusion of anion–anion repulsion via a Born type of potential, a value of $u = 0.304$ was found by minimizing the energy of a rutile geometry that, like ours, set all metal–oxygen distances equal. A more recent study by Baur[8] using a Lennard–Jones repulsive potential gave a value of $u = 0.306$ and a c/a ratio of 0.644 for a model that imposed no restrictions on the bond lengths.) Although such local arguments are often dangerous when it comes to understanding the results of Madelung calculations, it could be argued that the 4+/4+ metal–metal repulsions win out over the 2−/2− oxygen–oxygen repulsions in the unit shown in **5**. On a simple Coulombic repulsion model this gives rise to a considerably elongated edge-sharing octahedral chain along the z direction. Minimization of the Coulombic energy of the fragment shown in **5** as a function of angle gives a value of $\alpha = 32°$ to be compared with that found from a complete electrostatic crystal calculation of $\sim 36°$.

One feature of the structure that our calculation does not reproduce is the sense of the distortion away from the geometry where all Ti–O distances are set equal. **6** shows the results of a

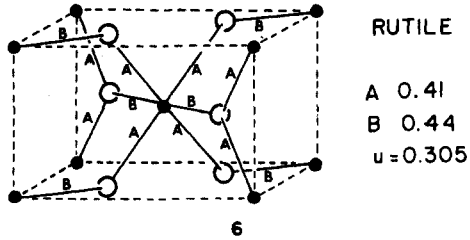

6

population analysis of the tight-binding wavefunctions determined at the minimum-energy geometry of Figure 2. Clearly, a structure with four long and two short metal–oxygen distances is predicted, which is the opposite to that actually found for TiO_2, where four distances of 1.946 Å and two distances of 1.984 Å are observed. (These overlap populations show a parallel decrease with increasing d count and never change in relative magnitude.) In accord with such a result, however, we calculate a stabilization (albeit a small one of about 0.5 kcal/TiO_2) on moving away from the energy minimum of Figure 2 along a coordinate with four long and two short Ti–O distances while keeping the average metal–oxygen distance constant. We also calculate a small destabilization for the analogous (opposite) distortion to the observed geometry. The energy changes associated with these two distortions are shown as dashed lines around the minimum of Figure 2. (We calculate that the energy change for an isolated TiO_6^{8-} unit undergoing such a geometrical change represents a stabilization of about half this value, irrespective of the sense of the distortion.) Notice from Table II that the energy sum underestimates both the destabilization on going to the observed structure and the stabilization on going to the lowest energy structure with the opposite distortion. Since the Ti–Ti (and O–O) distances within the chains decrease and increase respectively in these two distortions, it could be argued that the discrepancy is due to Ti–Ti repulsions, present in the full calculation but absent in the estimate via the energy sum. Specifically identifying the energetic contribution made by cation–cation repulsions is difficult. Obviously the method used to estimate the corresponding anionic interactions cannot be employed since the d^0 Ti atoms have no valence electrons. We have to resort to the less satisfactory method of identifying features that are dependent on the cation–cation distance. As a result we (perhaps unfairly) do not consider such interactions in as much detail as those we can estimate numerically.

In molecular chemistry, where overlap populations of idealized systems are often used to understand relative bond lengths in real systms, this technique has invariably been foolproof. The problem with rutile is interesting. For several years the sense of the distortions of the metal octahedron in rutile structures has been a puzzle. An ionic model (electrostatic forces plus Born repulsions) gives the result that the octahedron should contain two short and four long bonds.[8-10] This is, in fact, as long as Jahn–Teller distortions are ignored, observed for the transition-metal fluorides that adopt this structure. For the oxides, however, some have the reverse distortion of two long and four short distances (SnO_2, SiO_2, GeO_2, TiO_2, VO_2, MnO_2, and PbO_2) but three (CrO_2, RuO_2, and OsO_2) have the pattern found for the fluorides. This result has been used[9b] to suggest that TiO_2 etc. must be more "covalent" since the ionic model gives the wrong result. However our orbital model makes the wrong prediction too! Since the relative values of the overlap populations shown in **6** for the d^0 case are maintained for all d counts through d^{10} (The latter corresponds to SnO_2 (cassiterite), GeO_2, and SiO_2 (stishovite).), the fact that CrO_2 is ferromagnetic, and therefore a high-spin system, appears then on this model not to have anything to do with the sense of the octahedral distortion. It is interesting to note, however, that the electronic configurations of magnetic d^2 (CrO_2) and nonmagnetic d^4 (RuO_2 and OsO_2) bear an interesting relationship. The first occupies the same set of levels with electrons of the same spin that the second occupies with pairs of electrons.

We have performed a separate set of calculations on stishovite (SiO_2 in the rutile structure). The structure is an interesting one[9,11] since the O–O distances are short, especially the one corresponding to the shared octahedral edge (2.29 Å). There is a close Si–Si contact across this edge too. The distance is 2.67 Å, to be compared with a typical Si–Si single bond distance of 2.34 Å. Figure 4 shows the results of a set of calculations analogous to those of Figure 2, both for the full three-dimensional structure and for a single one-dimensional chain of edge-sharing octahedra. Notice that the distortion is associated with a larger energy change than that for the case of rutile TiO_2, as is to be expected since the oxide ions are closer together in SiO_2. A comparison of the value of u obtained from the minimum in either complete calculation and the smaller value predicted by the energetics of the oxide ion array

(6) Sahl, K. *Acta Crystallogr.* **1965**, *17*, 1027.
(7) (a) Pauling, L. "The Nature of the Chemical Bond"; Cornell University Press: Ithaca, NY, 1978. (b) Pauling, L. *Z. Kristallogr., Kristallgeom., Kristallphys., Kristallchem.* **1928**, *67*, 377.
(8) Baur, W. H. *Acta Crystallogr.* **1961**, *14*, 209.
(9) Baur, W. H.; Khan, A. A. *Acta Crystallogr., Sect. B: Struct. Crystallogr. Cryst. Chem.* **1971**, *B27*, 2133.
(10) Baur, W. H. *Acta Crystallogr., Sect. B: Struct. Crystallogr. Cryst. Chem.* **1976**, *B32*, 2200.
(11) Hill, R. J.; Newton, M. D.; Gibbs, G. V. *J. Solid State Chem.* **1983**, *47*, 185.

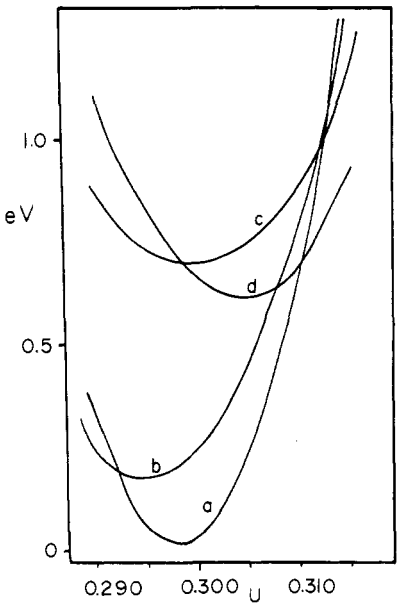

Figure 4. Results of band structure computations for stishovite as a function of u (energies per unit cell contents, namely two formula units): (a) tight-binding calculation for the full three-dimensional structure; (b) analogous calculation for the oxide ions only of part a; (c) tight-binding calculation for a one-dimensional chain of edge-sharing octahedra extracted from the crystal; (d) analogous calculation for the oxide ions only of part c.

indicates that a significant repulsion occurs between the silicon atoms in the structure. (Recall the lowest energy for the isolated SiO_6^{8-} unit will occur for the regular octahedron at $u = 0.293$.) Indeed a substantial negative Si–Si overlap population is found from our calculations. Such repulsions are ignored in the local treatment, but their effect clearly is to elongate the edge-sharing chains that run parallel to c. Such an effect is seen to be somewhat smaller for TiO_2 itself in Figure 2, although the OMO angle is virtually the same in the two real structures.

The overlap populations for the structure with regular octahedra (**7**) have the same relationship as those in TiO_2. These values

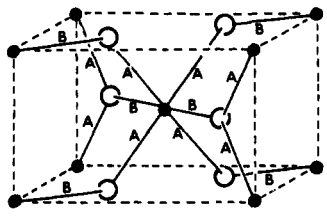

STISHOVITE

A 0.28

B 0.33

u=0.305

7

also predict the incorrect sense of the movement away from the idealized geometry. In stishovite, the silicon atom has four oxygen neighbors at 1.757 Å and two at 1.809 Å. However, the distortion in the opposite direction to that observed, and the one expected on the basis of these values, is associated with a (very small) destabilization. In a fashion similar to that found for TiO_2, a distortion of the structure with regular octahedra to the observed arrangement where the bond lengths are not equal is found to be destabilizing. Energetically the distortion is calculated to be $\approx$1 kcal/SiO_2, about twice as large as that for TiO_2. From Table II notice the unusual result that consideration of the energetics of the oxide lattice alone overestimates the magnitude of the energy change here but underestimates (the usual state of affairs for the structures of Table II) its magnitude for the opposite distortion. These two results are, of course, consistent with the presence of Si–Si repulsions, which decrease as the Si–O distance along the chain increases and are not included in the local calculations.

Now, what are these results concerning the finer details of the rutile structure telling us about the forces between the atoms in these solids? First, it is obvious that the energy changes we calculate via these computations are rather small. Second, it appears that the energetics are dominated by those of the oxide ion array, modified to some extent by what appear to be repulsions between the Ti or Si atoms. We could perhaps argue that the overlap-based, closed-shell repulsions between the oxide ions do not accurately mimic the finer details of the O–O pair potential. Since the finer details of the structure appear to be controlled by the energetics of the oxide matrix rather than by direct metal–oxygen interactions, the sense of the calculated overlap populations of the idealized geometry will then have little value in predicting the geometry of lowest energy. The results are analogous to those described for the Chevrel phases[3] where the Mo–Mo distances are tempered by anion–anion repulsions. However, there is more to this problem. The observed distortion around the oxide ion is, from experience with molecular chemistry, quite unusual. Unless the planar AB_3 unit is a low-spin d^8 species, then the sense of the distortion is always as shown in **8**. As the angle α decreases from

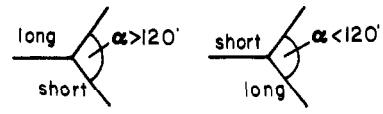

8

120; two long and one short distance are observed.[12] This result has a simple expanation in terms of sp mixing[13] in both molecular orbital and valence bond language. The distortion patterns shown in **8** are indeed those we would predict from the overlap populations derived from calculations on C_{2v} OTi_3^{10+} units where all the O–Ti distances are set equal (**9**). The calculated result for the solid

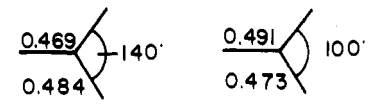

9

is then completely consistent with electronic ideas from molecules. They just happen to be contrary to the experimental results. For the time being then, the distortion of the idealized rutile structure remains a puzzle.

It is instructive to investigate in a little more detail the energetics of the local Ti and O geometries. This will allow an understanding of the energetic preference for the rutile structure for d^0 oxides. Eight-electron AB_3 molecules containing a first-row A atom are invariably pyramidal (e.g. NH_3 and NCl_3) but may be stabilized (**10**) in a planar geometry by the presence of good π-acceptor

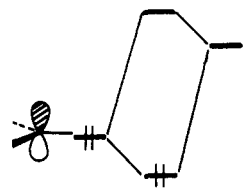

10

ligands[14] as in, for example, $N(SiH_3)_3$ (where the acceptor orbital is a low-lying σ^* orbital (**11**)). Similar comments apply to the stabilization of square-planar carbon by, for example, lithium atoms as described in ref 15. The empty d orbitals on Ti(IV) may play this role too, as shown in **12**. A similar effect stabilizes

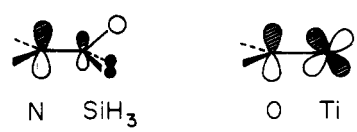

11 **12**

(12) Murray-Rust, P. "Abstracts of Papers", 3rd European Crystallography Meeting, 1976; p 206.
(13) Burdett, J. K. *Inorg. Chem.* **1979**, *18*, 1024.
(14) Albright, T. A.; Burdett, J. K.; Whangbo, M.-H. "Orbital Interactions in Chemistry"; Wiley: New York, 1985.
(15) Clark, T.; Schleyer, P. v. R. *J. Am. Chem. Soc.* **1979**, *101*, 7749.

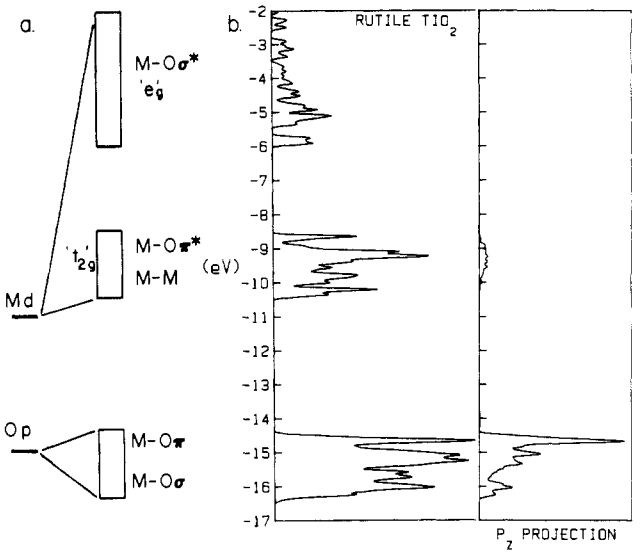

Figure 5. (a) Generation of the energy bands of rutile for an approximately octahedral metal environment and a trigonal-planar oxygen atom. (b) Density of states for rutile showing a projection of the p_z orbital (perpendicular to the plane) of the trigonal oxygen atom.

a square-planar oxygen atom in solid NbO and TiO.[16] There are also square-planar and butterfly-shaped OTi_4 units in some other early-transition-metal oxides. Maximum π overlap between metal d and oxygen p orbitals occurs at the planar structure, and hence maximum stabilization of the oxygen p_z orbital occurs at this geometry too. Some support for this π-bonding argument comes from consideration of the Ti–O distance in rutile itself. Pauling found[7a] this to be a full 0.1 Å shorter than predicted using a simple sum of his radii (but made no comment about this fact). There is a nice pictorial representation of the formation of the analogous Ti–C p–d_π bond (and a picture of the orbitals involved in the Ti–O bond) in ref 17. Energetically it is calculated to be worth ≈13 kcal/mol. Figure 5 shows the density of states we calculate for rutile TiO_2. The d band is split into the two blocks corresponding to the e_g and t_{2g} sets of the octahedron.[18] This means that the d^6 dioxides should be nonmetallic. This is in fact found to be the case for β-PtO_2. It has a resistivity of $\approx 10^6$ Ω cm.[19b] Also shown is the projection of the oxygen p orbital that lies perpendicular to the OTi_3 plane and is involved in π bonding with the relevant metal d orbitals from the t_{2g} set. Notice that the $p\pi$ orbital is not stabilized as much as the $p\sigma$ orbitals, and this gives rise to a characteristic spike in the density of states at the top of the oxygen p band. Notice too that the $p\pi$ character is located in the upper part of the "t_{2g}" band as expected from Figure 5a. Compare this plot with the corresponding one for NbO in ref 16. This p–$d\pi$ bonding becomes more pronounced on moving to the right of the transition-metal series. Since the oxygen p–metal d energy separation here is smaller than that at the left-hand side of the series, the interaction between them becomes larger. Our calculations show that a planar eight-electron OTi_3 unit (i.e. a d^0 metal) is strongly favored over a pyramidal geometry in accord with this argument. From Table II it is clear to see that the destabilization of the hexagonal eutactic structure is dominated by the instability of the nonplanar OTi_3 unit. For the same fragment in the cadmium iodide structure (vide infra) the geometry is considerably more pyramidal and the destabilization accordingly larger. An analogous effect contributes to an extra stabilization of the octahedral geometry at d^0 for the TiO_6 unit.

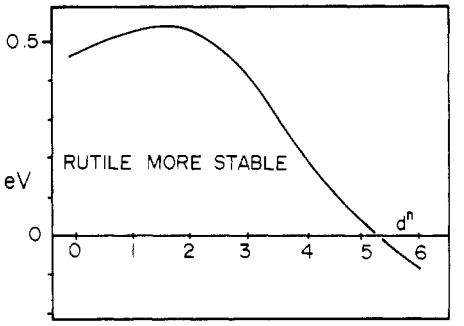

Figure 6. Energy difference curve between the rutile and $CaCl_2$ structures as a function of d count (energies per two formula units). The average Ti–O distance is set equal to 1.95 Å in both arrangements, and the observed crystallographic parameters (u, v of Table I) for rutile TiO_2 and PtO_2 were used.

From simple angular-overlap considerations,[20] the best π stabilization occurs when the triple degeneracy of the metal t_{2g} set is maintained and this will be for the regular octahedral structure.

With a nonzero d configuration the situation is different. Now M–O π^* levels may be occupied, and as the d count increases, the two-electron–two-orbital stabilization of the planar OTi_3 geometry is eventually replaced by a four-electron–two-orbital destabilization. Around d^2 (low spin) all the metal–oxygen π^* levels will be occupied and the planar geometry destabilized. Modeling this by using local OTi_3 units is difficult since there are a large number of Ti–O nonbonding (but not necessarily Ti–Ti nonbonding) orbitals in such a fragment. However increasing the electron count results in the pyramidal geometry eventually becoming the favored local arrangement. We cannot predict (without doing a calculation) at which d count the crossover in relative stability will occur, but it is interesting to note that, whereas IrO_2 (d^5) has the rutile structure, β-PtO_2 (d^6) does not.[19] It has the orthorhombic $CaCl_2$ arrangement with a nonplanar anion environment similar to that in **4**. (Parenthetically we note here that size arguments are no good to "rationalize" this observation. Examples of the rutile structure are known with cations whose radii are larger and smaller than that for platinum(IV).) Figure 6 shows the results of a set of band structure calculations designed to test these ideas. Plotted is the energy difference curve as a function of the number of d electrons for the β-PtO_2 structure (scaled so that the average bond length is 1.95 Å) and the minimum-energy (at d^0) TiO_2 rutile geometry. Quite apparent is the destabilization of the structure containing the planar oxygen atom, with d count and the crossover somewhere between d^5 and d^6, to the $CaCl_2$ structure. As the value of u in the reference rutile structure increases, the energetic penalty associated with the oxide ion array increases and the crossover point moves to lower d counts. With a value of $u \approx 0.305$ it occurs between d^4 and d^5. There is another way to pyramidalize the anion geometry in rutile. Recall that the marcasite structure, found for many metal disulfides from d^4 to d^8, is closely related to the rutile structure. Rotation of the MX_6 octahedra of rutile so that adjacent X atoms are brought close together leads to destruction of the planar X atom environment and generation of tetrahedral coordination about X, by three metal atoms and one X atom. The structure can now also be described in terms of M atoms and X_2 units.

For nonzero d counts the octahedral geometry around the metal atom is sometimes not the most favored one either. With partial occupation of the t_{2g} set, a Jahn–Teller distortion away from the octahedral structure of an isolated TiO_6 fragment is energetically favorable although the stabilization energy may not be very large. The distortion that is most advantageous for low-spin d^2 appears to be the one that takes the geometry with regular octahedra toward the geometry predicted to be the electrostatic minimum. We shall see below however that metal–metal bonding discourages this geometry for nonzero d counts. The presence of direct interactions between the metals also means that mimicking the

(16) Burdett, J. K.; Hughbanks, T. *J. Am. Chem. Soc.* **1984**, *106*, 3101.
(17) Hout, R. F.; Pietro, W. J.; Hehre, W. J. "A Pictorial Approach to Molecular Structure and Reactivity"; Wiley: New York, 1984.
(18) For some details of the band structure of these oxides see: Mattheiss, L. F. *Phys. Rev. B: Solid State* **1976**, *B13*, 2433.
(19) (a) Siegel, S.; Hoekstra, H. R.; Tani, B. S. *J. Inorg. Nucl. Chem.* **1969**, *31*, 3803. (b) Rogers, D. B.; Shannon, R. D.; Sleight, A. W.; Gillson, J. L. *Inorg. Chem.* **1969**, *8*, 841.
(20) Burdett, J. K. "Molecular Shapes"; Wiley: New York, 1980.

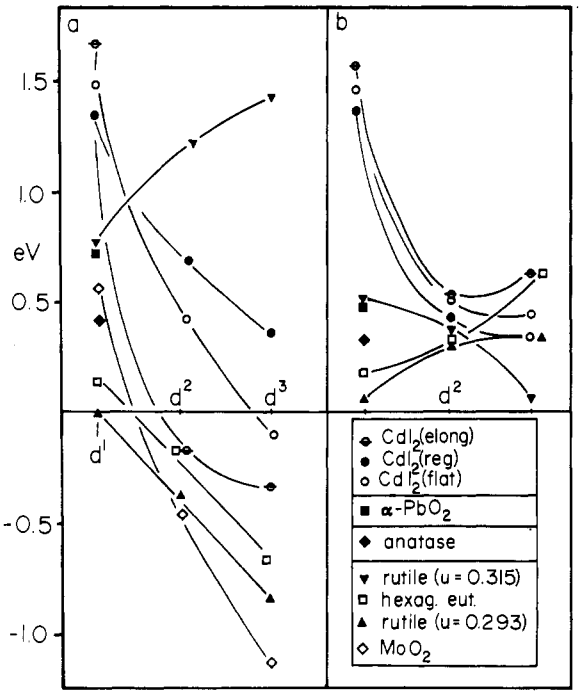

Figure 7. Energetics of several key crystal structures as a function of d count, relative to the minimum-energy geometry of curve a of Figure 2 (energies per two formula units): (a) results of tight-binding calculations on the crystalline materials; (b) estimates of the energies made by using a weighted sum of the energetics of the oxide ion array and contributions from local coordination environments. At the bottom of the figure is shown the separation of some of these structures into topologically distinct families.

energetics with local TiO_6 units is not very reliable either for nonzero d configurations.

Figure 7 shows the energetic behavior for d^{0-2} for a series of structures related to rutile in some way. In the left-hand panel are the computed energetics. In the right-hand panel are estimates for some key structures, made by summing the energetic variations in the local geometry contributions and that of the oxide lattice alone. Shown at the bottom of the figure in a diagrammatic way are four topological families. Within a given family structures may be interconverted without breaking bonds between metal and oxygen, but this is not true for structures in different families. The MoO_2 structure type is one whereby pairs of metal atoms within the edge-sharing chains of the rutile arrangement are brought together so that the metal–metal distances alternate along the chain. Such a distortion is accompanied by a twisting of these chains of octahedra too. Notice that the $CaCl_2$, MoO_2, and rutile structures belong to the same family and that the rutile arrangement, the only one from this series known for TiO_2, is indeed calculated to be the lowest energy structure at d^0. The anatase structure (a higher energy polymorph of TiO_2) lies in a different family. This structure may be vizualized as the cubic analogue of the α-PbO_2 structure (vide infra), where the Ti atoms are ordered over a cubic eutactic array of oxide ions. It results in the sharing of four edges per octahedron. (Interestingly one of the cubic analogues of rutile would be the cadmium chloride structure, where the strings of octahedra located within a pair of eutactic planes link up to share edges. This arrangement is just the cubic analogue of the cadmium iodide arrangement described below. The cubic framework structure analogous to rutile is not known.) Using a model with an average Ti–O distance of 1.95 Å, we calculate the anatase structure to lie 4.83 kcal/TiO_2 higher in energy than rutile. Thermochemical studies[21] have put this difference at 2.8 ±2 kcal/TiO_2. Our calculations (Table II) indicate that both local geometry and matrix penalties contribute to this effect. This result is an interesting one since anatase is

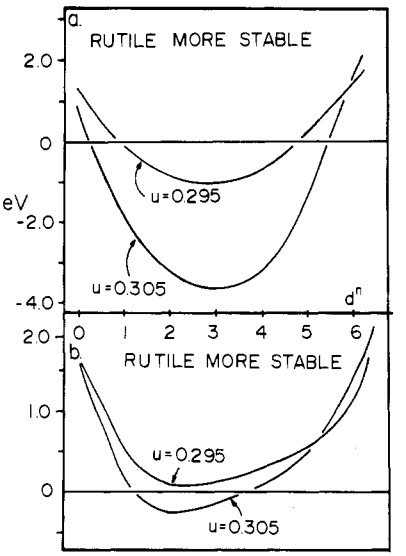

Figure 8. (a) Difference in energy (calculated for TiO_2) between the rutile and MoO_2 structures, the latter with the same average Ti–O distance as used for rutile (1.95 Å). (b) Same as part a but using metal parameters (appropriate for iron) that are less diffuse. (Energies are given per two formula units.)

a less dense structure than rutile (by about 10%). Clearly then, not always is the maximum volume structure the most stable. Anatase also has a smaller Madelung constant[7a] than rutile, a consequence of both a less dense structure and the presence of more shared edges per octahedron.

The MoO_2 Structure

Several early-transition-metal dioxides, namely d^1 VO_2 (at lower temperatures), d^2 MoO_2 and WO_2, and d^3 α-ReO_2 and TcO_2, exhibit[19b] a structure in which the metal atoms are paired up along the z axis of the tetragonal rutile unit cell (**13**). (For VO_2 the

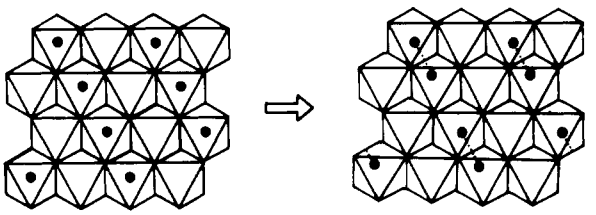

13

structure at 300 K is the usual rutile one, and the actual details of how such a Peierls type of structural distortion proceeds as the temperature is lowered is quite complex.[22]) Figure 8a shows the energy differences we calculate for TiO_2 for the observed MoO_2 structure[23] (scaled so that the average Ti–O distance is 1.95 Å) vs. those calculated for the rutile structure with d count, assuming that all the electrons are paired. Two curves are shown. One corresponds to the rutile structure with a u parameter equal to 0.295, which leads to a metal–metal distance of 2.80 Å. The other with u = 0.305 results in a Ti–Ti distance of 2.91 Å. The average metal–metal distance in the scaled MoO_2 structure used in the calculated is 2.75 Å. The energy difference curves are very typical ones[12] and show increasing stabilization as metal–metal-bonding orbitals (formed from the "t_{2g}" block) are filled (d^0–d^3) and then destabilization as antibonding levels are filled (d^4–d^6). Opposing the effects of metal–metal bonding are the unfavorable lattice and local geometrical contributions discussed above, which means that at d^0 and d^6 the rutile arrangement must be more stable. The MoO_2 structure is predicted to be the favored geometry for

(21) "JANAF Thermodynamic Tables", *Natl. Stand. Ref. Data Ser. (U.S. Natl. Bur. Stand.)* **1971**, *NSRDS-NBS 37*.

(22) Pouget, J. P.; Launois, H.; Rice, T. M.; Dernier, P.; Gossard, A.; Villeneuve, G.; Hagemuller, P. *Phys. Rev. B: Solid State* **1974**, *B10*, 1801.

(23) Murphy, D. W.; DiSalvo, F. J.; Carides, J. N.; Waszcak, J. V. *Mater. Res. Bull.* **1978**, *13*, 1395.

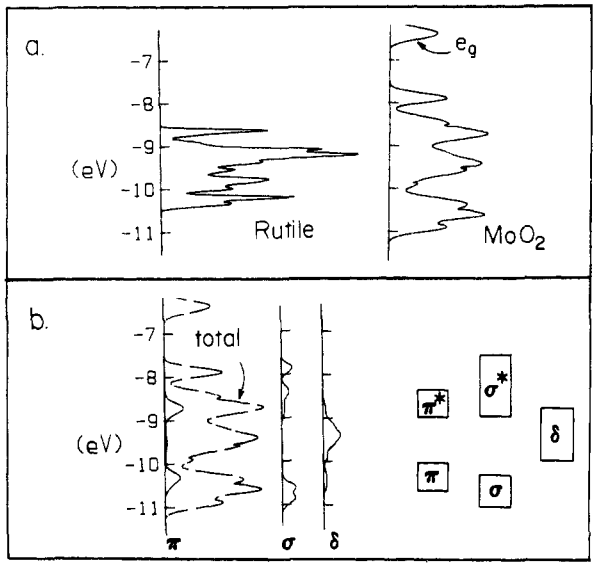

Figure 9. (a) Change in the density of states of the regular rutile structure on distortion to the MoO_2 arrangement. (b) Projection of σ, π, and δ components from the density of states and the generation of a block diagram describing the metal–metal interaction. The δ band gains negligible width from metal–metal overlap. Its width arises almost entirely from π bonding with the oxide ligands.

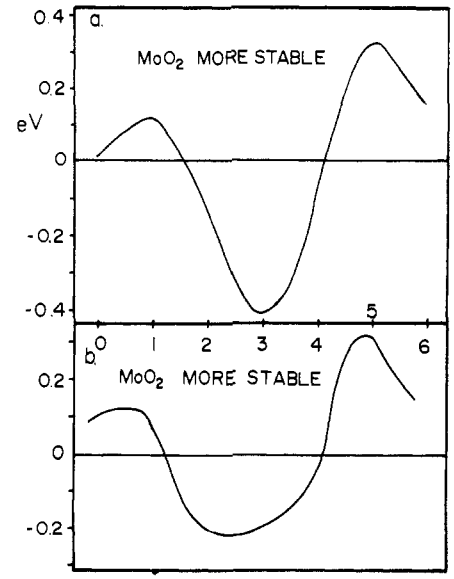

Figure 10. Energy difference between the one-dimensional building blocks of the rutile and α-PbO_2 structures shown in **15** as a function of the number of d electrons (energies per two formula units): (a) curve for the undistorted arrangement; (b) curve for the case where the metal atoms have been paired.

nonmagnetic d^{1-4} systems, although for d^1 there is only a very small stabilization with respect to the rutile structure with $u = 0.295$. This would correspond to the interesting case of VO_2, for which see our discussion above. For first-row dioxides where the "t_{2g}" band may be narrow compared to electron–electron repulsion energies, a high-spin system is possible. CrO_2 and MnO_2 are, in fact, ferromagnetic and antiferromagnetic, respectively. Since population of metal–metal-antibonding orbitals is more energetically unfavorable for the MoO_2 structure, these two oxides are found in the rutile arrangement. The heavier congeners of these two elements form nonmagnetic dioxides with the MoO_2 structure.

Figure 9a shows how the rutile density of states changes on distortion to the MoO_2 structure. Notice the broadening of the "t_{2g}" band as a result of decreasing some of the metal–metal distances. In Figure 9b we project the contribution from relevant combinations of metal d orbitals that have σ, π, and δ symmetry with respect to the metal–metal linkage. (For an octahedron in the usual orientation sharing edges along x, these would be the $x^2 - y^2$, xz, and yz orbitals, respectively.) These projections give rise to the block diagram of the band structure shown at the far right-hand side. There are clearly σ, π, σ^*, and π^* "bands". The δ band gains most of its width from π type interactions with the oxide ions. This picture is similar[24] to many others obtained via pairing distortions of one-dimensional chains, such as those in $NbCl_4$[25] and $BaVS_3$.[26] These systems contain isolated chains built from edge- and face-sharing octahedra, respectively.

On moving to the right of the periodic table metal atoms become smaller. In electronic terms their d orbitals become less diffuse. Figure 8b shows energy difference curves analogous to those of Figure 8a using metal orbital parameters appropriate for iron. Notice the smaller energetic effect of these contracted d orbitals and also that the minima in these curves have shifted from d^3 to d^2. We will not describe in any detail how this comes about, but the shift is the result of a change in the order of filling the bands equivalent to those in Figure 9b. When one moves to a system where the M–M interaction is weaker, the π and π^* bands are not split apart as in Figure 9b. As a consequence of this, whereas σ and π are full at d^2, the next electron starts to fill π-antibonding levels as well as the nonbonding δ band.

With these more contracted metal parameters, and $u = 0.295$, the MoO_2 arrangement is less stable than the rutile structure for all d counts. Relative to the rutile structure with $u = 0.305$ (and a longer metal–metal distance), the MoO_2 arrangement is calculated to be more stable for d^2 and d^3 only. Our results here are consistent with (but of course do not prove) the view that undistorted rutiles are to be found for $d^{4,5}$ because of weaker metal–metal interaction. (For d^5, metal–metal bonding is less stabilizing than for d^1 since antibonding orbitals are destabilized more than the corresponding bonding orbitals are stabilized and this will be a contributary effect.) $d^{2,3}$ oxides should exhibit the strongest distortions from Figure 8, a result in accord with the observed c/a ratios in these systems.[19b] Tight-binding calculations such as ours are not very reliable when it comes to reproducing the detailed energetics associated with bond length changes, and so we have not searched for the global energy minimum associated with the rutile/MoO_2 pair of structures.

The α-PbO_2 Structure

The α-PbO_2 structure is closely related to that of rutile. Half of the octahedral holes of a pair of hexagonal eutactic layers of oxide ions are filled with metal atoms such that zigzag chains (rather than the straight chains of rutile) are produced (**14**). This

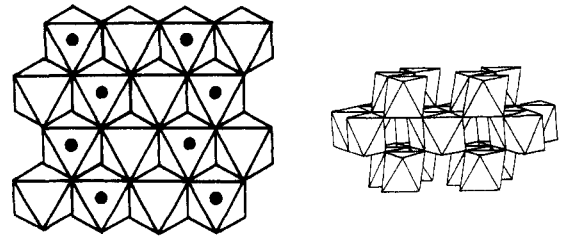

14

structure is calculated to be about 0.38 eV/TiO_2 higher in energy than the lowest energy rutile arrangement. this energetic difference is dominated by an unfavorable packing of the oxide ions, which are significantly distorted away from hexagonal eutaxy. In a previous study of these systems[27] we were unable to ascribe the energy difference between these two structures to local geometry effects but needed to use a much larger fragment of the structure, a result in accord with the arguments used here. This

(24) Burdett, J. K. *Prog. Solid State Chem.* **1984**, *15*, 173.
(25) Whangbo, M.-H.; Foshee, M. J. *Inorg. Chem.* **1981**, *20*, 113.
(26) Whangbo, M.-H.; Foshee, M. J.; Hoffmann, R. *Inorg. Chem.* **1980**, *19*, 1723.
(27) Burdett, J. K.; Haaland, P.; McLarnan, T. J. *J. Chem. Phys.* **1981**, *75*, 5764.

particular form of TiO_2 has been observed[28] after unloading a sample of rutile that has been subjected to high pressure.[29] Intriguing is the report of orthorhombic (β) ReO_2 (d^3) with this structure but with the metal atoms paired.[30] The structural relationships in eq 3 are useful to remember. Figure 10 shows

$$\begin{array}{l} \text{rutile} \text{———} MoO_2 \\ \alpha\text{-}PbO_2 \text{———} \beta\text{-}ReO_2 \end{array} \quad (3)$$

the energy difference curve we calculate for the two idealized systems shown in **15**, which are the building blocks for the rutile

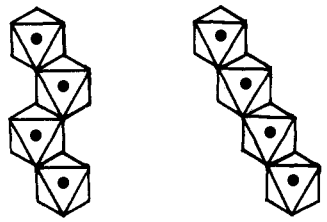

15

and α-PbO_2 structures. Note the simple (and as we will point out very characteristic) form of this energy difference curve. Interestingly the maximum stabilization of the α-PbO_2 structure occurs at d^3 (i.e. ReO_2). Figure 10 also shows the analogous energy difference curve for the two distorted units where the metals have been moved together in pairs. A similar calculation using the experimentally determined coordinates for β-ReO_2 and for MoO_2 (but scaling the structures so that the average Ti–O distance is 1.95 Å) shows a more pronounced stabilization of the β-ReO_2 structure at d^3, in accord with the very short metal–metal distance in the real structure.

Elsewhere we describe, using the method of moments, how curves such as that of Figure 10a arise in general.[31] This particular plot is a characteristic one for two systems whose first disparate moment in the energy density of states is the fourth. We can generate the nth moment of the "t_{2g}" energy density of states by enumerating the number of walks of length n among the xz, yz, and xy orbitals of the system and weighting each step by the corresponding interaction integral.[31] Most of the walks of length 4 are the same in the two structures, but there are two critical ones that are different. For simplicity of presentation, if we assume that the edges that shared in the α-PbO_2 structure are the cis edges (rather than the skew edges) of the octahedron, then these walks are those shown in **16** and **17**. The walk shown

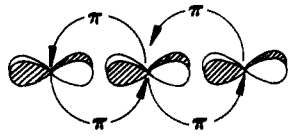

16

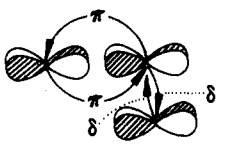

17

in **16** is weighted by β_π^4, but the corresponding one in **17** is only weighted by $\beta_\pi^2\beta_\delta^2$. Since δ interactions are much weaker than π type interactions, the rutile arrangement has the larger fourth moment. A similar argument applies to the real structure. Accordingly,[31] it is the structure that will be maximally stabilized at the one-fourth- and three-fourths-filled band. The α-PbO_2 structure, with the smaller fourth moment, will be maximally stabilized at the half-filled band (i.e. d^3). A similar argument can be envisioned for the two distorted structures. In view of these remarks it might be interesting to search for α-PbO_2 or β-ReO_2 dioxides with d^2 or d^4 configurations. Our argument here, although phrased in a somewhat novel way, is, in fact, basically the same[14] as that for skew (rather than planar) O_2F_2, for staggered (rather than eclipsed) *trans*$(CH_2CH_2)_2ML_4$ complexes, and for the perpendicular arrangement of the CH_2 groups in allene.

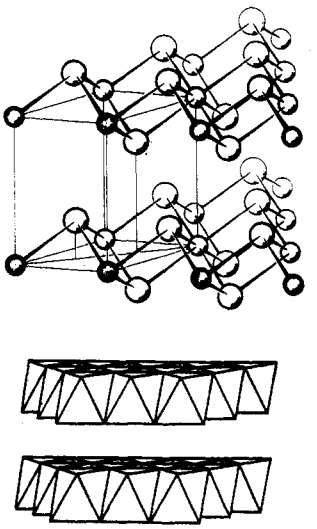

Figure 11. The cadmium iodide structure.

Cadmium Iodide and Molybdenite (MoS_2)

The energetic importance of the geometry at oxygen is strikingly apparent when the calculated energy of the cadmium iodide (Figure 11) structure is compared with that of rutile. In this layer structure, the octahedral holes between hexagonal eutactic layers of oxides are alternately all full and all empty. This leads to pyramidal coordination at the oxygen atom but with a local C_{3v} geometry (**18**) compared to the C_s geometry present in the $CaCl_2$

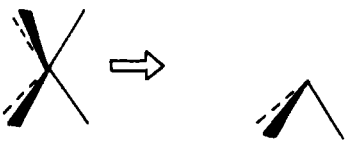

18

structure (**3**, **4**). Our comments here will also apply to the cadmium chloride structure, where the anions are arranged in cubic rather than hexagonal eutaxy. Decreasing the c/a ratio of such a structure leads to a flattening of the oxygen geometry whereas the converse leads to an increase in pyramidality. As may be seen in Table II, the instability of this arrangement of d^0 is almost entirely due to the local energetics at the anion, the difference becoming smaller as the c/a ratio decreases. The hollandite and diaspore structures, adopted for example by α- and γ-MnO_2, may be regarded geometrically as lying between the rutile and cadmium halide structures. In view of our assessment of the energetics of the systems in local terms, we should expect these species to lie energetically between these two extremes. It has been suggested[32] that these structures are only found in practice because of their stabilization by small amounts of cation impurity in the channels.

The cadmium halide structure has an extra degree of freedom (as does molybdenite below) in which the anion sheets that do not enclose metal atoms may split apart. Obviously our calculations include no van der Waals forces that will stop this happening. In fact we only calculate a small stabilization ($\approx$0.06 eV/TiO_2) for this process, since the eutactic lattice contains no unfavorable contacts. In TiS_2 with this structure,[33] the interlayer anion spacings are virtually identical irrespective of whether the layers sandwich metal atoms or not.

(28) Liu, L. G. *Science* (*Washington*, D.C.) **1978**, *199*, 422.
(29) Although the α-PbO_2 arrangement containing this zigzag motif is calculated to be of higher energy than rutile for TiO_2, this structural unit is a common fundamental building block in many structures. An example that contains such linked TiO_6 octahedra is ramsayite, $Na_2Ti_2Si_2O_9$: Chin-Khan; Simonov, M. A.; Belov, N. V. *Dokl. Acad. Nauk. SSSR* **1969**, *186*, 820.
(30) Magneli, A. *Acta Crystallogr.* **1956**, *9*, 1038; *Acta Chem. Scand.* **1957**, *11*, 28.
(31) (a) Burdett, J. K.; Lee, S. *J. Solid State Chem.*, in press. (b) *J. Am. Chem. Soc.*, in press.
(32) Clark, M. G. "The Structures of Non-Molecular Solids"; Applied Science: Barking, England, 1972.
(33) (a) Chianelli, R. R.; Scanlon, J. C.; Thompson, A. H. *Mater. Res. Bull.* **1975**, *10*, 1379. (b) For a study on TiS_2 itself and how it is modified by donor intercalates, see: Whangbo, M.-H.; Rouxel, J.; Trichet, L.; Gressier, P. *Inorg. Chem.*, in press.

The molybdenite (MoS_2) structure (**19**) is analogously desta-

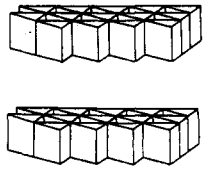

19

bilized at d^0 relative to rutile. Here, as in cadmium iodide, the local anion geometry is pyramidal. Also, since the eutactic sheets of oxide ions are stacked as eclipsed pairs, the repulsions between them are larger than in the hexagonal eutactic case. Furthermore, the trigonal-prismatic coordination of the metal engendered by such an arrangement is unfavorable at d^0. This structure is then energetically unfavorable on all three counts at d^0. Neither the cadmium halide nor molybdenite structure is known for any d^0 MO_2 system. Of the structures we have mentioned, only the three lower energy ones, namely rutile, anatase, and α-PbO_2, are known. (There are other known structures that we have not tackled in this paper, among them the brookite form of TiO_2 with three shared edges per octahedron. It is based on a double hexagonal eutaxy of anions and so is geometrically intermediate between rutile and anatase.)

How do the results change with d count? Recall that as the metal–oxygen π^* levels start to be filled, the pyramidal geometry at oxygen becomes less energetically penalized compared to that of the planar arrangement. Notice in Figure 7 how the cadmium halide structure is rapidly stabilized as a result. Also, it is now the elongated structure that lies lowest in energy. This is the one with the most pyramidal oxygen. However, metal–metal bonding is extremely important in these species too. A comparison of the curves in Figure 7a,b indicates that, as might be expected, the stabilization from this source increases with decreasing metal–metal distance. (See the footnotes to Table I.) Numerically, from our computations its variation appears to be of the same order of magnitude as that of all of the other effects combined. (But recall our cautionary note above concerning the difficulty of accurately assessing the planar/pyramidal energy difference with d count and the lack of a good quantitative agreement on our model.) The cadmium iodide structure with the ions in hexagonal eutaxy has the same metal–metal distance as hexagonal eutactic rutile. Elongation of this structure brings the metal atoms more closely together. A prediction of which structure lies lowest in energy is difficult since the details of the energetic interplay of metal–metal interactions (attractive for low d counts), O–O interactions (repulsive), and angular geometry changes about the anion and cation sites are crucial. Also, we would expect that, as the d count increases, the occupation of metal–ligand π-antibonding orbitals will result in a change in anion–cation distance. We have noted that estimation of the energetic changes associated with bond length variations is one of the weakest features of the extended Hückel method, and we feel that a numerical method better than ours is required to provide the correct balance. Also, as we discuss elsewhere,[34] one usually finds in structures with these d counts clustering of the collection of metal atoms within a basic structure type. Such distorted structures are invariably close in energy when studied with our numerical method. In fact between d^1 and d^3 examples are known of oxides of rutile, anatase, MoO_2, hollandite, diaspore, cadmium halide, and molybdenite types.[34] Some of these are only known as stuffed derivatives. For example, the titanium and oxygen atoms in $Li_{0.5}TiO_2$ are found in the anatase arrangement.[35] In this light we note too that α- and γ-MnO_2 (vide supra) are always[36] nonstoichiometric (metal rich), but the β form (rutile type) is a stoichiometric material. Certainly the effect of the electropositive stuffing atom is not to be ignored in structure discrimination.

Other Systems

It is of interest to enquire how these conclusions are modified when the oxide ion is replaced by other ions A. If A is not a first-row atom, of paramount importance is the result that now the ATi_3 unit is more stable in the pyramidal geometry than in the planar one for all metal d counts. The analogous comparison[12] to make for the molecular situation is between $N(SiH_3)_3$ and $P(SiH_3)_3$. The former is planar (vide supra), but the latter is pyramidal (Si–P–Si = 96°). π bonding to second-row atoms is less important energetically than bonding to first-row atoms. Also, the σ part of the interaction between the central atom and the ligands, which stabilizes the pyramidal geometry, as measured by the inversion barrier in the binary hydrides, increases markedly on going from NH_3 (6 kcal/mol) to PH_3 (≈33 kcal/mol). As a direct result of this reversal, it is now the cadmium halide structure that is the preferred arrangement at d^0 when oxide is replaced by chalcogenide. This is the structure experimentally found for TiS_2[33] and ZrS_2. In fact, the rutile structure is not stable for MX_2 species for any electron count if X is other than a first-row atom. (But see our comments above concerning the relationship between rutile and marcasite structures.) It is not impossible to produce a planar environment at phosphorus or sulfur. See[39] for example the molecule $Cp_2Hf(PEt_2)_2$. Our thesis is that it is energetically more difficult than for first-row atoms. At d^2 the trigonal-prismatic arrangement is stabilized compared to the octahedral geometry (a well-known result from coordination chemistry[37]), and the molybdenite structure (which also contains pyramidal sulfur atoms) now becomes a possibility. It is, of course, found for MoS_2 (d^2) itself.[38] By the use of these ideas, it is then quite understandable why the cadmium halide structures are also found for many transition-metal chlorides, bromides, and iodides and why the calcium chloride structure is found for many heavier group 2 halides,[42] although we cannot at present energetically discriminate between these two structures. The transition-metal difluorides that universally adopt the rutile structure of a Jahn–Teller distorted variant for d counts from 2 through 10 are systems where π bonding involving the very electronegative fluorine atom is probably negligible. For these species then we suspect the energetics are dominated by the anion array. Local geometry energetic contributions are small by comparison, and the rutile structure is found for all d counts.

Our explanation of the essential difference between oxygen and sulfur in terms of π bonding and the stiffness of the σ framework,[12] although a useful one, is not the only way to tackle the problem of the lowest energy oxygen or sulfur geometry. Hyde and O'Keeffe have suggested[40a] that the geometry is simply determined by nonbonded repulsions around the two- or three-coordinate center. In other words, a through-bond mechanism has been replaced by a through-space mechanism. The oxygen atom with short linkages to its neighbors allows them to approach closely if the angle is too small. Nonbonded repulsions are then supposed to be responsible for the opening of Si–O–Si angles to 149°, on average, and by extension to keep the OTi_3 unit planar. For heavier central atoms, with longer bond lengths, such nonbonded repulsions are presumed to be negligible and much tighter angles, those demanded by the electronic requirements of the central atom, are found. It is easy to dismiss the nonbonded argument as an important factor *on our model* since all of the local geometry calculations were performed on molecules where interactions between the ligands have been switched off and it is the anionic and not the cationic lattice we have chosen as our matrix. But we often find significant negative (i.e. repulsive) overlap popu-

(34) Burdett, J. K.; Hughbanks, T. *Inorg. Chem.*, in press.
(35) Cava, R. J.; Murphy, D. W.; Zahurak, S.; Santoro, A.; Roth, R. S. *J. Solid State Chem.* **1984**, *53*, 64.
(36) Glemser, O.; Gattow, G.; Meisick, H. *Z. Anorg. Allg. Chem.* **1961**, *309*, 20.
(37) (a) Kertesz, M.; Hoffmann, R. *J. Am. Chem. Soc.* **1984**, *106*, 3453. (b) Hoffmann, R.; Howell, J. M.; Rossi, A. R. *J. Am. Chem. Soc.* **1976**, *98*, 2484.
(38) An energy difference curve for rutile and molybdenite oxides as a function of d count is given in ref 34.
(39) Baker, R. T.; Whitney, J. F.; Wreford, S. S. *Organometallics* **1983**, *2*, 1049.
(40) (a) O'Keeffe, M.; Hyde, B. G. *Trans. Am. Crystallogr. Assoc.* **1979**, *15*, 65. (b) Hyde, B. G.; O'Keeffe, M. *Nature (London)* **1984**, *309*, 411.

Table III. Atomic Parameters

atom	orbital	H_{ii}, eV	exponent
O	2s	-26.0	2.275
	2p	-16.0	2.275
Si	3s	-17.3	1.383
	3p	-9.2	1.383
Ti	4s	-8.97	1.50
	4p	-5.44	1.50
	3d[a]	-10.81	4.55 (0.4391), 1.60 (0.7397)
Fe	4s	-10.97	1.75
	4p	-7.44	1.75
	3d[a]	-12.81	5.35 (0.5505), 2.00 (0.6260)

[a] Double-ζ functions with coefficients in parentheses.

lations between the ligands in calculations where these interactions were retained. Indeed we described above a significant effect of the silicon-silicon repulsions in stishovite. Recently Hyde and O'Keeffe have presented[40b] an interesting view of the existence or nonexistence of solid-state structures using these ideas.

We may extend the orbital arguments presented above past the transition-metal series to the elements of groups 13 and 14.[42] The orbitals for example in SiH_3, which may be identified as having the correct symmetry and energy to act as acceptor orbitals after the style of **10**, are the σ^* orbitals shown in **11**. In phosphines (PR_3) these are the orbitals that make this ligand an excellent π acceptor when coordinated to a transition metal. For GeO_2, SnO_2 (cassiterite), and SiO_2 (stishovite), we can imagine a similar coupling of a low-lying M-O σ^* orbital at each Ge, Sn, or Si that can stabilize the planar oxygen in a similar way. Recall in this light that SnS_2 has the cadmium iodide structure. (GeS_2 and SiS_2 have structures containing four-coordinate cations.) In an analogous fashion such orbitals may stabilize the planar nitrogen atoms in Ge_3N_4 and Si_3N_4. We reserve comment on the stabilization of linear oxygen by such a mechanism for a separate publication.[2]

Acknowledgment. We thank the donors of the Petroleum Research Fund, adminstered by the American Chemical Society, for partial support of this research. It was also supported by the National Science Foundation via NSF Grant DMR8019741. Thanks are also due to Dr. T. Hughbanks for his assistance with some of the calculations and for several useful discussions.

Appendix

All the computations were carried out by using a program employing the extended Hückel model, which may be used for both molecular and crystal calculations. (See ref 24 for a discussion of the orbital links between the energy levels of finite and infinite molecules.) It has been developed to its present state by M.-H. Whangbo, S. Wijeyesekera, M. Kertesz, C. N. Wilker, and T. Hughbanks, and the decomposition of the energy density decomposition of states shown in Figure 9 is now routine. The crystal calculations were performed for a large enough **k**-point set to achieve energetic self-consistency. Typically for rutile, a set of 40 points corresponding to the irreducible wedge of the primitive tetragonal Brillouin zone was used.

Ti-O distances of 1.95 Å were employed throughout, except for those systems where more than one Ti-O distance was permitted by symmetry. In such cases this value represented the average Ti-O distance. Si-O distances were analogously fixed at 1.77 Å, close to the mean distance in stishovite.[11] With knowledge of the u parameter, this specifies all the geometrical details for the rutile structure. Computations on the MoO_2, PtO_2, β-ReO_2, and α-PbO_2 structures employed the fractional coordinates of ref 23, 19a, 30, and 41, respectively. The orbital parameters are shown in Table III. The modified weighted Wolfsberg-Helmholz equation was used to estimate the interaction integrals.

(41) Wykoff, R. G. W. "Crystal Structures"; Wiley: New York, 1973.
(42) In this paper the periodic group notation is in accord with recent actions by IUPAC and ACS nomenclature committees. A and B notation is eliminated because of wide confusion. Groups IA and IIA become groups 1 and 2. The d-transition elements comprise groups 3 through 12, and the p-block elements comprise groups 13 through 18. (Note that the former Roman number designation is preserved in the last digit of the new numbering: e.g., III → 3 and 13.)

Contribution from the Institut de Chimie Physique, Ecole Polytechnique Fédérale, CH-1015 Lausanne, Switzerland

Dynamics of Interfacial Charge-Transfer Reactions in Semiconductor Dispersions. Reduction of Cobaltoceniumdicarboxylate in Colloidal TiO_2

ULRICH KÖLLE,[1] JACQUES MOSER, and MICHAEL GRÄTZEL*

Received November 2, 1984

The dynamics of electron transfer from the conduction band of colloid TiO_2 solutions in water to cobaltoceniumdicarboxylate $[Co(C_5H_4COO)_2]^-$ (**1**) were investigated by using laser photolysis to excite the semiconductor. The decay of the blue color of the electron in the TiO_2 particle as well as the formation of the 484-nm absorption of $[Co(C_5H_4COO)_2]^{2-}$ was used to monitor the course of the reaction. At pH 10, the electron spectrum has a maximum at 780 nm and its extinction coefficient at this wavelength has been determined as 800 M^{-1} cm^{-1}. The rate of reduction is controlled by the interfacial charge-transfer step. The unique pH effect on the rate constant can be understood in terms of simultaneous protonation of the two carboxylate groups of the reduced acceptor. In acidic solution **1** affords a drastic (up to 50-fold) enhancement of interfacial conduction band electron transfer to other acceptors such as viologens.

Introduction

In a previous communication[2] we have introduced cobaltoceniumdicarboxylate (**1**) as a new redox mediator for light energy conversion devices. Subsequent experiments showed that this electron acceptor is superior to methylviologen when used in aqueous chloroplast suspensions as a relay compound for hydrogen generation[3] or in regenerative photoelectrochemical cells based

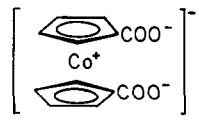

1

on p-InP semiconductor electrodes.[4] Advantages of this mediator are its high chemical stability[5] and relatively weak visible light absorption in both the oxidized and the reduced form. In neutral

(1) Visiting scientist from the Institut für Anorganische Chemie, Technische Hochschule, D-5100 Aachen, West Germany.
(2) Houlding, V.; Geiger, T.; Kölle, U.; Grätzel, M. *J. Chem. Soc., Chem. Commun.* **1982**, 682.
(3) Cuendet, P.; Grätzel, M. *Photochem. Photobiol.* **1982**, *36*, 203.
(4) Geiger, T.; Nottenberg, T.; Pélaprat, M.-L. *Helv. Chim. Acta* **1982**, *65*, 2507.
(5) Sheats, J. E. *J. Organomet. Chem. Libr.* **1979**, *7*, 461.

0020-1669/85/1324-2253$01.50/0